

# Electromagnetically induced transparency and reduced speeds for single photons in a fully quantized model

Thomas Purdy<sup>1,3</sup> and Martin Ligare<sup>2,4</sup>

<sup>1</sup> Department of Physics, Carnegie Mellon University, Pittsburgh, PA 15213, USA

<sup>2</sup> Department of Physics, Bucknell University, Lewisburg, PA 17837, USA

E-mail: mligare@bucknell.edu

Received 11 October 2002, in final form 10 March 2003

Published 29 May 2003

Online at [stacks.iop.org/JOptB/5/289](http://stacks.iop.org/JOptB/5/289)

## Abstract

We introduce a simple model for electromagnetically induced transparency in which all fields are treated quantum mechanically. We study a system of three separated atoms at fixed positions in a one-dimensional multimode optical cavity. The first atom serves as the source for a single spontaneously emitted photon; the photon scatters from a three-level ‘ $\Lambda$ ’-configuration atom which interacts with an additional single-mode field coupling two of the atomic levels; the third atom serves as a detector of the total transmitted field. We find an analytical solution for the quantum dynamics. From the quantum amplitude describing the excitation of the detector atom we extract information that provides exact single-photon analogues to wave delays predicted by semi-classical theories. We also find complementary information in the expectation value of the electric field intensity operator.

**Keywords:** Electromagnetically induced transparency, group velocity, phase velocity, quantized field, scattering

## 1. Introduction

Controlling the phase coherence in ensembles of multilevel atoms has led to the observation of many striking phenomena in the propagation of near-resonant light. These phenomena include coherent population trapping, lasing without inversion, electromagnetically induced transparency, and anomalously slow and anomalously fast pulse velocities. Resonant enhancement of the index of refraction without an accompanying increase in absorption was proposed [1] and observed [2, 3] in 1991, and drastic reductions in the group velocity of pulses were discussed shortly thereafter [4]. Recent experiments have taken the reduction of the speed of light to extreme limits [5, 6] and at the other extreme lie observations of seemingly superluminal light [7, 8]. An overview of recent developments in the control of photons is presented in [9]. An earlier review of electromagnetically induced transparency

was presented by Harris [10], while Lukin *et al* present an overview of phase coherence in general with an extensive list of references [11]. Such effects are also discussed in recent texts (see, for example [12]). In most previous work the phenomenon of electromagnetically induced transparency and the accompanying drastic slowing of the speed of light are treated using semi-classical theory in which the atoms of the medium are treated quantum mechanically and the fields are treated classically. We use a model in which the entire system is treated quantum mechanically, and study the propagation of a field state containing a single photon. Although coherent states of a single mode quantized field are often considered as the ‘most classical’, the multimode single photon states that we study exhibit striking parallels with classical fields. The model we present is idealized, and does not correspond to the conditions of a specific experiment. We present it in an effort to provide interpretive clarity at the quantum level of electromagnetically induced transparency and anomalously slow light speeds.

We study a system of three separated atoms at fixed positions in a one-dimensional multimode optical cavity. The

<sup>3</sup> Current address: Department of Physics, University of California, Berkeley, CA 94720-7300, USA.

<sup>4</sup> Author to whom any correspondence should be addressed.

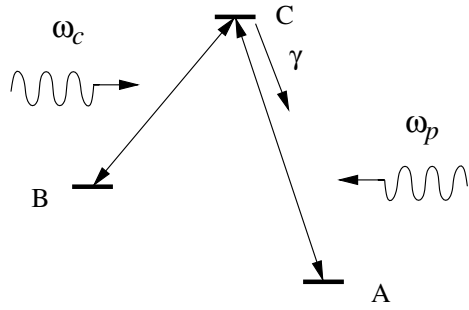


**Figure 1.** Level scheme for simple electromagnetically induced transparency. A strong field resonantly couples levels B and C, and weak probe is near resonance with the transition between levels A and C. The upper level C decays via spontaneous emission to the ground state A; other damping mechanisms are assumed to be negligible.

first atom serves as the source for a single spontaneously emitted photon; the photon scatters from a three-level ‘ $\Lambda$ ’-configuration atom which interacts with an additional single-mode field coupling two of the atomic levels; and the third atom serves as a detector of the total transmitted field. In the spirit of Feynman’s derivation of the classical index of refraction from the interaction of a field with a single oscillator [13], we infer the properties of a medium exhibiting electromagnetically induced transparency from the interaction of the spontaneously emitted quantum field with the single quantized scattering atom. We find an analytical solution for the quantum dynamics, including reradiation from the scatterer, and from this we deduce quantum delays that characterize the propagation of the field. These delays are equivalent to those predicted by semi-classical theories. In our quantum model all delays are clearly the result of interfering amplitudes that reshape the temporal envelope of the probability of detecting the transmitted photon. This effect is most clearly illustrated in the graphs of detection probability versus time displayed in section 5. This work is an extension of the model we have used previously to study quantum manifestations of classical wave delays induced by scattering from simple two-level atoms [14]. We note that the analytical results obtained in this paper may be verified using straightforward numerical techniques like those used in [15–18].

## 2. Review of semi-classical theory

Electromagnetically induced transparency can be observed in the simple three-level atom illustrated in figure 1. A strong ‘coupling’ laser with angular frequency  $\omega_c$  is tuned to resonance with the transition between atomic levels B and C, while a weak ‘probe’ laser with angular frequency  $\omega_p$  excites the transition between levels A and C. In this paper we consider the simplest case in which decay from levels C to B is small enough to be neglected, and the only damping is due to emission at a rate  $\gamma$  from level C to the ground state A. (In this paper all decay rates  $\gamma_j$  refer to decay of probability of finding the atom in the excited state.) We also assume that there is no incoherent pumping driving population between the levels of the atom.

In the limit of a weak probe the complex susceptibility is given by [12]

$$\chi = \left( \frac{N|d|^2}{\hbar\epsilon_0} \right) \frac{\delta}{\omega_R^2/4 - \delta^2 - i\delta\gamma/2}, \quad (1)$$

where  $N$  is the density of the atoms,  $d$  is the dipole moment of the transition between levels A and C,  $\omega_R$  is the Rabi frequency of the coupling transition between levels B and C, and the detuning of the probe laser frequency from resonance with the transition between levels A and C is

$$\delta = \omega_p - \omega_{AC}. \quad (2)$$

The index of refraction and the absorption coefficient can be calculated from the real and imaginary parts of the complex susceptibility, respectively. When the probe field is resonant with the transition between levels A and C, i.e.  $\delta = 0$ , the absorption goes to zero and the index of refraction is a rapidly varying function of probe frequency.

For later comparison with the results of our quantum model, we consider a classical monochromatic plane wave of frequency  $\omega_p$  which is normally incident on a thin slab containing atoms with the level structure illustrated in figure 1. The plane of the slab is normal to the  $z$  axis, the thickness of the slab is  $\Delta z$ , and the density of the atoms is  $N$ . If the incident field is  $E_i = E_0 \exp[-i\omega(t - z/c)]$ , the transmitted field on the far side of the slab is

$$E_t = E_i \exp\left(i \frac{\omega_p \chi \Delta z}{2c}\right), \quad (3)$$

and for weak scattering the transmitted field is approximately

$$E_t \simeq E_i \left[ 1 + i f \frac{\delta\gamma/2}{\omega_R^2/4 - \delta^2 - i\delta\gamma/2} \right], \quad (4)$$

where we have introduced the small dimensionless parameter  $f = N\Delta z|d|^2\omega_p/(\hbar\epsilon_0 c\gamma)$  characterizing the magnitude of the scattering.

The dispersion in the response of the atoms in this model leads to delays of pulses traversing such a slab. The delay in the arrival of the peak of a modulation envelope of a quasi-monochromatic pulse is determined by the group velocity  $v_g = d\omega/dk = c/(n + \omega \frac{dn}{d\omega})$ , and is given by

$$\Delta t_g = \frac{\Delta z}{v_g} - \frac{\Delta z}{c} = \frac{\Delta z}{c} \left( n - 1 + \omega \frac{dn}{d\omega} \right). \quad (5)$$

For detunings such that  $\delta \ll \omega_{AC}$  the group delay is

$$\Delta t_g = 2f\gamma \frac{(\omega_R^2 + 4\delta^2)[(\omega_R^2 - 4\delta^2)^2 - 4\gamma^2\delta^2]}{[(\omega_R^2 - 4\delta^2)^2 + 4\gamma^2\delta^2]^2}. \quad (6)$$

The functional form of the delay when  $\omega_R = \gamma/2$  is illustrated in figure 2. When the probe field is resonant with the transition between levels A and C the group velocity can be extremely small, and this is manifested in the large positive group delay at  $\delta = 0$  in figure 2. The central peak in figure 2 becomes taller and narrower as the strength of the coupling field is reduced. We note that for some values of the detuning  $\delta$  the group delay is negative, which corresponds to group velocities greater than the vacuum speed of light,  $c$ . Such ‘superluminal’ velocities

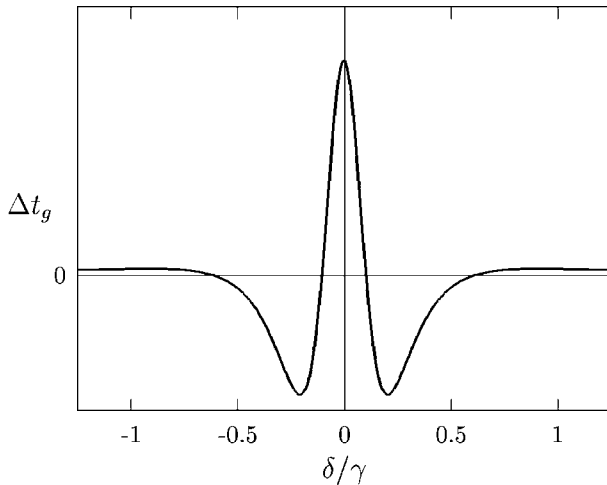


**Figure 2.** Group delay for a classical pulse in a medium with susceptibility given by equation (1). The strength of the coupling field is such that  $\omega_R = \gamma/2$ .

do not violate causality, and are an effect of pulse reshaping and intensity redistribution by the dispersive medium. Similar reshaping effects and group velocities greater than  $c$  occur near simple two-level resonances in both classical and quantum theories.

For pulses that are insufficiently monochromatic the simple concepts of phase and group velocity are inadequate for characterizing all of the effects of pulse reshaping as the field propagates. Several other velocities and delays have been developed (see, for example, [19, 20]) and in this paper we focus on a delay determined by the ‘temporal centre-of-gravity’ of the field intensity of a pulse at a fixed position  $z$  ‘downstream’ from the slab containing the atoms comprising the medium, i.e.

$$\Delta t_{\mathcal{E}^2} = \left( \frac{\int t \mathcal{E}(z, t)^2 dt}{\int \mathcal{E}(z, t)^2 dt} \right)_{\text{after medium}} - \left( \frac{\int t \mathcal{E}(z, t)^2 dt}{\int \mathcal{E}(z, t)^2 dt} \right)_{\text{vacuum}}. \quad (7)$$

This is closely related to concepts used to define the centrovlocity in [19]. We have investigated this delay in classical and quantum mechanical models of scattering from simple two-level atoms in a previous paper [14]. For quasi-monochromatic pulses far from resonance this delay is equivalent to the group delay, but in general it is necessary to calculate explicitly the field  $\mathcal{E}$  in order to determine  $\Delta t_{\mathcal{E}^2}$ . As in our previous study [14], the ‘temporal-centre-of-gravity’ delay provides a framework for an unambiguous and causal interpretation of delays in both classical and quantum models. For the specific pulses with Lorentzian spectrums under consideration, we will show that the ‘temporal-centre-gravity’ delay is identical to twice the group delay.

### 3. Quantum mechanical model

The quantum mechanical system under consideration is illustrated in figure 3, and consists of three atoms at fixed positions in a multimode one-dimensional optical cavity that extends from  $z = 0$  to  $L$ . This multimode cavity is oriented horizontally in the schematic representation of figure 3. The middle atom has an additional interaction with a single-mode

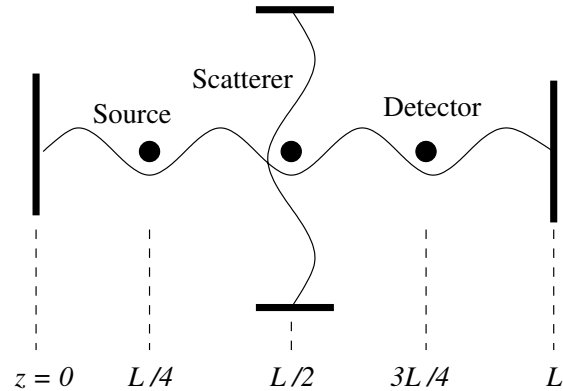


**Figure 3.** Quantum mechanical model consisting of three atoms at fixed positions. All three atoms interact with the radiation in the probe field in the *multimode* cavity (represented horizontally) and the middle atom also interacts with the single mode coupling field (represented vertically).

field contained in the vertical cavity. The field in the multimode (horizontal) cavity plays the role of the probe field, and the field in the single mode (vertical) cavity represents the coupling field. The probe cavity is assumed to be large in the sense that the length  $L$  is very much greater than the wavelength of the light emitted by the atoms. (The finite optical cavities do not contribute to the physical phenomena under investigation; they simply provide a convenient quantization volume for the field modes used in our calculation.) In the remainder of this section we will discuss the details of our model and the standard quantum optical Hamiltonian we use. We also present the analytical solution for the time dependence of the system.

The atom on the left (atom 1) is a two-level atom which is initially in the excited state, and will be the source of the probe field. The middle atom (atom 2) which will scatter the radiation emitted by the source is a three-level atom with the ‘ $\Lambda$ ’-configuration of figure 1, and the energy difference between levels A and C is close to that of the level separation of atom 1. (The highest level of all three atoms will be labelled as C.) Levels B and C of atom 2 will interact with the single-mode coupling field which is assumed to be exactly on resonance. The coupling field will initially be in a state with a well defined number of photons such that the Rabi frequency of the transition between levels B and C is appropriate for the observation of electromagnetically induced transparency. The two-level atom on the right (atom 3) will serve as a detector. The detector atom is assumed to have the same resonant frequency as the source atom. The relative energy levels of all three atoms are illustrated in figure 4.

No assumption is made about the relative strength of the three atoms’ coupling to the field, so that atoms have distinct decay rates. Although we find a solution for the dynamics for any set of decay rates, we focus our attention in this paper on cases in which the decay rate of atom 1 is very much smaller than the decay rate of atom 2. This condition insures that the spectrum of the radiation emitted by atom 1 will be very much narrower than the line-width of the scattering atom, and this allows us to compare our results from the quantum case with those of the semi-classical model which assumes that the sample is driven by a monochromatic wave. We also focus on cases when the decay rate of the detector atom (atom 3) is very

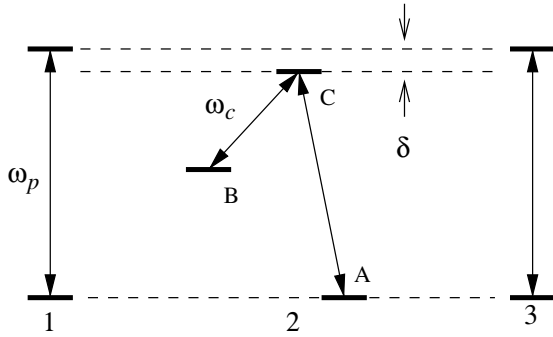


**Figure 4.** Level scheme of the source, scattering, and detector atoms. The source and detector are two-level atoms with identical transition frequencies. The scattering atom is a three-level atom in the ‘ $\Lambda$ ’ configuration. The transition frequency of the source and detector are detuned from the A–C transition of the scattering atom by an amount  $\delta$ .

much greater than any other dynamical rates in the problem. In this limit the excitation of atom 3 will closely follow the field that drives it. For simplicity we also assume that the spontaneous decay rate from level C to level B (for atom 2) is negligible. This is, of course, an idealization; in the modelling of real experiments it is necessary to account for such decays. As mentioned in the introduction, our goal in this paper is interpretive clarity in the context of a fully quantized model, and assuming that this decay is negligible makes our quantum analysis tractable. It is straightforward to include this decay in a semi-classical model like that presented in [12].

The zero-field resonance frequencies of the A–C transitions of the atoms are labelled  $\omega_j^{(\text{at})}$ , where  $j = 1, 2$ , or 3, and the positions of the atoms will be labelled  $z_j$ . In the remainder of the paper we will assume that the atoms are at positions  $z_1 = L/4$ ,  $z_2 = L/2$ , and  $z_3 = 3L/4$ , as illustrated in figure 3, although our results for delay times do not depend on the exact positions. The standing wave field modes of the probe field cavity are separated in angular frequency by the fundamental frequency

$$\Delta = \pi \frac{c}{L}. \quad (8)$$

This mode spacing may be small enough that many modes fall within the natural line-width of the atoms.

For convenience we assume that the frequency of one of the modes corresponds exactly to the resonance frequency of atom 1, the emitting atom, and that the length of the cavity is such that it contains an even number of wavelengths of this mode. We label the frequency of this mode  $\omega_0 = m_0\Delta$ , where  $m_0$  is an integer divisible by 4. (This assumption affects the details of some of our calculations, but not our results concerning delay times.) The other mode frequencies will be enumerated from this mode so that

$$\omega_m = (m_0 + m)\Delta, \quad (9)$$

where  $m = 0, \pm 1, \pm 2, \dots$

As in the semi-classical case we wish to study the effects of the detuning of the source field on the scattering of the radiation. We use the same symbol  $\delta$  as in the semi-classical case to represent the detuning of the field, but in the quantum

case the detuning is directly tied to the properties of the source and scattering atoms

$$\delta = \omega_1^{(\text{at})} - \omega_2^{(\text{at})}. \quad (10)$$

Owing to the fact that the detector atom is assumed to have the same resonance frequency as the source atom we have  $\omega_1^{(\text{at})} = \omega_3^{(\text{at})}$ .

We use as basis states the eigenstates of the atomic plus free-field Hamiltonian

$$\begin{aligned} \hat{H}_0 &= \hat{H}_{\text{atoms}} + \hat{H}_{\text{field}} \\ &= \hat{H}_{\text{atoms}} + \hat{H}_{\text{probe}} + \hat{H}_{\text{coupling}} \\ &= \hbar\omega_1^{(\text{at})}|C_1\rangle\langle C_1| + \hbar\omega_2^{(\text{at})}|C_2\rangle\langle C_2| + \hbar(\omega_2^{(\text{at})} - \omega_c)|B_2\rangle\langle B_2| \\ &\quad + \hbar\omega_3^{(\text{at})}|C_3\rangle\langle C_3| + \sum_m \hbar\omega_m a_m^\dagger a_m + \hbar\omega_c a_c^\dagger a_c, \end{aligned} \quad (11)$$

where  $a_m$  and  $a_m^\dagger$  are the lowering and raising operators for the  $m$ th mode of the probe field, and  $a_c$  and  $a_c^\dagger$  act similarly on the single mode of the coupling field. (We have re-zeroed the energy scale to remove zero-point energy of the field modes.) The basis states will be denoted as follows:

- $|C, A, A; 0, N\rangle$ —Atom 1 excited, atoms 2 and 3 in ground state A, no photons in the probe field,  $N$  photons in the coupling mode;
- $|A, C, A; 0, N\rangle$ —Atom 2 in state C, atoms 1 and 3 in ground state A, no photons in the probe field,  $N$  photons in the coupling mode;
- $|A, A, C; 0, N\rangle$ —Atom 3 excited, atoms 1 and 2 in ground state A, no photons in the probe field,  $N$  photons in the coupling mode;
- $|A, A, A; 1_m, N\rangle$ —All atoms in ground state A, one photon in the probe field mode with frequency  $(m_0 + m)\Delta$ ,  $N$  photons in the coupling mode;
- $|A, B, A; 0, N + 1\rangle$ —Atom 2 in state B, atoms 1 and 3 in ground state A,  $N + 1$  photons in the coupling field.

We use the standard electric-dipole and rotating-wave approximations in the interaction Hamiltonian [21] to give

$$\begin{aligned} \hat{H}_{\text{int}} &= \sum_{j=1}^3 \sum_m \hbar(g_{jm} a_m^\dagger |A_j\rangle\langle C_j| + g_{jm}^* a_m |C_j\rangle\langle A_j|) \\ &\quad + \hbar(g_c a_c^\dagger |B_2\rangle\langle C_2| + g_c^* a_c |C_2\rangle\langle B_2|), \end{aligned} \quad (12)$$

where the strength of the coupling of the  $j$ th atom to the  $m$ th mode of the probe field is characterized by the constant  $g_{jm}$ . The Rabi frequency  $\omega_R$  of the transition between levels B and C is determined by the number of photons in the coupling mode and the coupling constant  $g_c$  as follows:

$$\omega_R = 2g_c \sqrt{N + 1}. \quad (13)$$

For convenience we assume that  $\omega_R$  is real.

We assume that the frequencies of all atomic transitions are very much greater than the fundamental frequency of the cavity, i.e.  $\omega_j^{(\text{at})} \gg \Delta$ , and similarly for  $\omega_c$ . In this limit we can make the approximation that all modes that influence the dynamics of the system are near the atomic resonances, and the atom–field coupling constants are given by

$$g_{jm} = \Omega_j \sin[(m_0 + m)\pi z_j / L]. \quad (14)$$

In this equation  $\Omega_j$  is a constant given by

$$\Omega_j = d_j \left( \frac{\omega_j^{(\text{at})}}{2\hbar\epsilon_0 V} \right)^{1/2}, \quad (15)$$

where  $d_j$  is the dipole matrix element between levels A and C of atom  $j$ , and  $V$  is the effective volume of the cavity.

We assume that the system begins in the state with the source atom excited, and the coupling field in a well defined number state, i.e.

$$|\psi(0)\rangle = |C, A, A; 0, N\rangle, \quad (16)$$

and write the time-dependent state of the system as the linear combination

$$\begin{aligned} |\psi(t)\rangle = & c_1(t)|C, A, A; 0, N\rangle + c_2(t)|A, C, A; 0, N\rangle \\ & + c_3(t)|A, A, C; 0, N\rangle + d(t)|A, B, A; 0, N+1\rangle \\ & + \sum_m b_m(t)|A, A, A; 1_m, N\rangle. \end{aligned} \quad (17)$$

(In real experiments it is difficult to prepare a state with a well defined photon number like the initial state of the coupling field that we have assumed; more realistic photon states are built as linear combinations of such Fock states. The evolution of each term in such a linear combination will be given by the solution derived in this paper, with the value of  $N$  appropriate for the term. If the spread in the values of the Rabi frequency of the A–B transition determined by the range of photon numbers is small compared to the frequency itself, the results will not differ appreciably from those given for an initial state of the form of equation (16).)

Choosing the zero of the energy scale at the level of (uncoupled) state  $|C, A, A; 0, N\rangle$ , the Schrödinger equation yields the following set of coupled differential equations:

$$\dot{c}_1 = -i \sum_m g_{1m} b_m, \quad (18)$$

$$\dot{c}_2 = -i \left( \sum_m g_{2m} b_m + \omega_R d/2 - \delta c_2 \right), \quad (19)$$

$$\dot{c}_3 = -i \sum_m g_{3m} b_m, \quad (20)$$

$$\dot{d} = -i(\omega_R c_2/2 - \delta d), \quad (21)$$

$$\dot{b}_m = -i \left( \sum_j g_{jm}^* c_j + m \Delta b_m \right). \quad (22)$$

We solve this set of equations with the Laplace transform technique used by Stey and Gibberd [22]. Laplace transforms have also been used to solve the Schrödinger equation in similar problems with two interacting atoms in three dimensions [23, 24] and in our own recent work on scattering from two-level atoms [14]. Because the Laplace transform technique is not new, and because we would like to focus on analogies with the fields in the semi-classical model and physical interpretation, we leave the details of our solution to the appendix, and simply quote our results here.

The general features of the solution giving the time dependencies of the atomic excitation amplitudes are illustrated in figure 5. The initially excited atom decays exponentially until  $t = 0.5L/c$ , the time at which scattered and

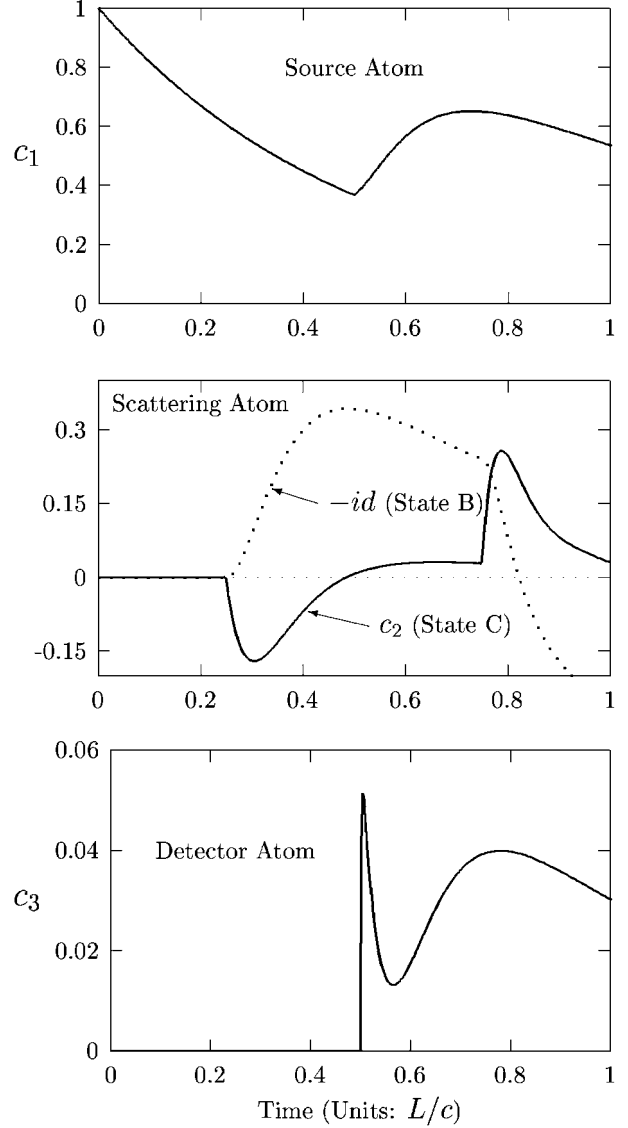


**Figure 5.** Magnitude of the amplitudes for the atoms to be in the excited state, starting from the state  $|\psi(0)\rangle = |C, A, A; 0, N\rangle$ . The decay rates of the atoms are  $\gamma_1 = 4$ ,  $\gamma_2 = 64$ , and  $\gamma_3 = 1024$  in the units of the figure; the Rabi frequency of the B–C transition of atom 2 is  $\omega_R = \gamma_2/2 = 32$ , and  $\delta = 0$ .

reflected radiation first returns to the atom. The amplitudes to find the other atoms excited are identically zero until radiation first reaches them: the scattering atom first becomes excited at  $t = 0.25L/c$  and the detector atom is first excited at  $t = 0.5L/c$ . The three decay constants which characterize the spontaneous emission rates of level C in each of the atoms emerge naturally in terms of the parameters of the Hamiltonian as

$$\gamma_j = \frac{\pi |\Omega_j|^2}{\Delta} = |\Omega_j|^2 \frac{L}{c}. \quad (23)$$

The causal nature of the dynamics is evident in that all disturbances are propagated at the speed of light  $c$  via the quantum field. The abrupt changes in the complex amplitudes at intervals of  $0.5L/c$  are a manifestation of the finite speed of light and the atomic spacing of  $0.25L$ .

The abrupt changes appear in our analytic solution for the complex amplitudes  $c_j(t)$ ,  $d(t)$ , and  $b_m(t)$  as sums of terms with step functions that ‘turn on’ at successively later intervals of  $0.5L/c$ . In the following formulae giving these amplitudes we truncate the expressions so that only the first excitations of atoms 2 and 3 are included. We also note that the following equations are specific in some details to the atomic positions  $z_i$  used in this paper. The positions of the atoms enter via the coupling constants  $g_{jm}$ , and changes in positions will result in changes in ‘turn-on’ times and relative phases of terms. The initial atomic decay rates given by equation (23) are *not* affected by the positions of the atoms; the effects of position dependence in the coupling constants compensate to keep the total decay rates independent of position. Our large-cavity limit  $\omega \gg \Delta_c$  means the atoms have time to decay at their free-space rates before interruption by reflected and scattered radiation. (Examples of the relationship between interrupted free-space decay and modified decay rates are given in [25].) The conclusions of this paper concerning delay times are unaffected by any details of position dependence.

The explicit time dependence of the system is given by the following set of amplitudes, in which we use the labels  $\mathcal{F}_i$  as a shorthand for complicated coefficients that are functions of  $\gamma_i$ ,  $\delta$ ,  $\omega_R$ , and (in the case of  $b_m$ ),  $m$ , and in which the time is scaled in units of  $L/c$ :

$$c_1(t) = \exp\left(-\frac{\gamma_1}{2}t\right) + \Theta\left(t - \frac{1}{2}\right) \left( \exp\left[-\frac{\gamma_1}{2}\left(t - \frac{1}{2}\right)\right] \times [\mathcal{F}_1 + (t - \frac{1}{2})\mathcal{F}_2] + \exp\left\{\left[-\left(\gamma_2 - \sqrt{\gamma_2^2 - 4\omega_R^2}\right)/4 + i\delta\right]\left(t - \frac{1}{2}\right)\right\} \mathcal{F}_3 + \exp\left\{\left[-\left(\gamma_2 + \sqrt{\gamma_2^2 - 4\omega_R^2}\right)/4 + i\delta\right]\left(t - \frac{1}{2}\right)\right\} \mathcal{F}_4 \right) + \dots, \quad (24)$$

$$c_2(t) = \Theta\left(t - \frac{1}{4}\right) \left( \exp\left[-\frac{\gamma_1}{2}\left(t - \frac{1}{4}\right)\right] \mathcal{F}_5 + \exp\left\{\left[-\left(\gamma_2 - \sqrt{\gamma_2^2 - 4\omega_R^2}\right)/4 + i\delta\right]\left(t - \frac{1}{4}\right)\right\} \mathcal{F}_6 + \exp\left\{\left[-\left(\gamma_2 + \sqrt{\gamma_2^2 - 4\omega_R^2}\right)/4 + i\delta\right]\left(t - \frac{1}{4}\right)\right\} \mathcal{F}_7 \right) + \dots, \quad (25)$$

$$c_3(t) = \Theta\left(t - \frac{1}{2}\right) \left( \exp\left[-\frac{\gamma_1}{2}\left(t - \frac{1}{2}\right)\right] \mathcal{F}_8 + \exp\left\{\left[-\left(\gamma_2 - \sqrt{\gamma_2^2 - 4\omega_R^2}\right)/4 + i\delta\right]\left(t - \frac{1}{2}\right)\right\} \mathcal{F}_9 + \exp\left\{\left[-\left(\gamma_2 + \sqrt{\gamma_2^2 - 4\omega_R^2}\right)/4 + i\delta\right]\left(t - \frac{1}{2}\right)\right\} \mathcal{F}_{10} + \exp\left[-\frac{\gamma_3}{2}\left(t - \frac{1}{2}\right)\right] \mathcal{F}_{11} \right) + \dots, \quad (26)$$

$$d(t) = \Theta\left(t - \frac{1}{4}\right) \left( \exp\left[-\frac{\gamma_1}{2}\left(t - \frac{1}{4}\right)\right] \mathcal{F}_{12} + \exp\left\{\left[-\left(\gamma_2 - \sqrt{\gamma_2^2 - 4\omega_R^2}\right)/4 + i\delta\right]\left(t - \frac{1}{4}\right)\right\} \mathcal{F}_{13} + \exp\left\{\left[-\left(\gamma_2 + \sqrt{\gamma_2^2 - 4\omega_R^2}\right)/4 + i\delta\right]\left(t - \frac{1}{4}\right)\right\} \mathcal{F}_{14} \right) + \dots, \quad (27)$$

$$b_m(t) = \left[ \exp\left(-\frac{\gamma_1}{2}t\right) - \exp(-im\pi t) \right] g_{1m} \mathcal{F}_{15} + \Theta\left(t - \frac{1}{4}\right) g_{2m} \left( \exp\left[-\frac{\gamma_1}{2}\left(t - \frac{1}{4}\right)\right] \mathcal{F}_{16} + \exp[-im\pi(t - \frac{1}{4})] \mathcal{F}_{17} + \exp\left\{\left[-\left(\gamma_2 - \sqrt{\gamma_2^2 - 4\omega_R^2}\right)/4 + i\delta\right]\left(t - \frac{1}{4}\right)\right\} \mathcal{F}_{18} + \exp\left\{\left[-\left(\gamma_2 + \sqrt{\gamma_2^2 - 4\omega_R^2}\right)/4 + i\delta\right]\left(t - \frac{1}{4}\right)\right\} \mathcal{F}_{19} \right) + \dots \quad (28)$$

Complete expressions for the factors  $\mathcal{F}_i$  are available from the authors.

Four rates are manifest in the exponential factors in these equations: the exponential decay rate of the source atom  $\gamma_1$ , which we will assume to be small, the exponential decay rate of the detector atom  $\gamma_3$ , which we will assume to be large, and two decay rates associated with the scattering atom,  $2\gamma'_2 \equiv \gamma_2 + \sqrt{\gamma_2^2 - 4\omega_R^2}$  and  $2\gamma''_2 \equiv \gamma_2 - \sqrt{\gamma_2^2 - 4\omega_R^2}$ . When the coupling field strength is small, the last of these rates approaches zero. This potential for slow reradiation is essential for the existence of the reduced velocities which characterize media with electromagnetically induced transparency. The resonant behaviour which determines the relative contributions of reradiation at the various rates is contained in the coefficients  $\mathcal{F}_i$ .

In the following sections we will focus on two quantities:  $c_3(t)$ , the amplitude to find the detector atom excited, and  $\langle \hat{\mathcal{E}}^2 \rangle$  the expectation value of the square of the electric field operator, which is proportional to the field intensity. (The expectation value of the field operator itself is zero for any state with the form of equation (17).) In our investigation of  $c_3(t)$  we will consider only the displayed term in equation (26) describing the initial excitation of the detector atom. Similarly, we will investigate  $\langle \hat{\mathcal{E}}^2 \rangle$  in regions to the right of the scattering atom, and at times that exclude multiple scattering effects.

It is useful to rewrite  $c_3(t)$  as the sum of two pieces: the amplitude  $c_3^0(t)$  for atom 3 to be excited in the absence of the scattering atom (or, equivalently, when  $\gamma_2 = 0$ ), and  $c_3^s(t)$ , the amplitude that is attributable to scattering. The total amplitude is thus

$$c_3(t) \equiv c_3^0(t) + c_3^s(t). \quad (29)$$

Setting  $\gamma_2 = 0$  in equation (26) gives

$$c_3^0(t) = \Theta\left(t - \frac{1}{2}\right) \frac{\sqrt{\gamma_1 \gamma_3}}{\gamma_1 - \gamma_3} \left\{ \exp\left[-\frac{\gamma_1}{2}\left(t - \frac{1}{2}\right)\right] - \exp\left[-\frac{\gamma_3}{2}\left(t - \frac{1}{2}\right)\right] \right\}, \quad (30)$$

and subtracting this from equation (26) gives

$$c_3^s(t) = \Theta\left(t - \frac{1}{2}\right) \left\{ \exp\left[-\frac{\gamma_1}{2}\left(t - \frac{1}{2}\right)\right] \mathcal{F}_{20} + \exp\left[-\left(\frac{\gamma_2''}{2} + i\delta\right)\left(t - \frac{1}{2}\right)\right] \mathcal{F}_{21} + \exp\left[-\left(\frac{\gamma_2'}{2} + i\delta\right)\left(t - \frac{1}{2}\right)\right] \mathcal{F}_{22} + \exp\left[-\frac{\gamma_3}{2}\left(t - \frac{1}{2}\right)\right] \mathcal{F}_{23} \right\}, \quad (31)$$

where

$$\mathcal{F}_{20} = \frac{\sqrt{\gamma_1 \gamma_3}}{(\gamma_1 - \gamma_3)} \frac{\gamma_2(\gamma_1 + i2\delta)}{\gamma_1^2 - \gamma_1 \gamma_2 - 4\delta^2 + \omega_R^2 + i2\delta(2\gamma_1 - \gamma_2)}, \quad (32)$$

$$\mathcal{F}_{21} = \left( \frac{\gamma_1 \gamma_3}{\gamma_2^2 - 4\omega_R^2} \right)^{1/2} \frac{\gamma_2 \gamma_2''}{(\gamma_1 - \gamma_2'' + i2\delta)(\gamma_3 - \gamma_2'' + i2\delta)}, \quad (33)$$

$$\mathcal{F}_{22} = \left( \frac{\gamma_1 \gamma_3}{\gamma_2^2 - 4\omega_R^2} \right)^{1/2} \frac{\gamma_2 \gamma_2'}{(\gamma_1 - \gamma_2' + i2\delta)(\gamma_3 - \gamma_2' + i2\delta)}, \quad (34)$$

$$\mathcal{F}_{23} = \frac{\sqrt{\gamma_1 \gamma_3}}{(\gamma_1 - \gamma_3)} \frac{\gamma_2(\gamma_3 + i2\delta)}{\gamma_3^2 - \gamma_2 \gamma_3 - 4\delta^2 + \omega_R^2 + i2\delta(2\gamma_3 - \gamma_2)}. \quad (35)$$

As an alternative to finding the time dependence of the excitation amplitude for the detector atom, we can characterize the transmitted field itself without recourse to the details of the detector. Standard photodetection theory [12] suggests calculation of the expectation value  $\langle \hat{\mathcal{E}}^{(-)}(z, t) \hat{\mathcal{E}}^{(+)}(z, t) \rangle$ , where  $\hat{\mathcal{E}}^{(+)}(z, t)$  and  $\hat{\mathcal{E}}^{(-)}(z, t)$  correspond to the decomposition of the interaction representation field operator into positive and negative frequency parts. This is equivalent to the calculation of the expectation value of the normally ordered intensity operator ( $\hat{\mathcal{E}}^2$ ).

Using the electric field operator in the form given in [21], we write the expectation value of the square of the field as

$$\langle : \hat{\mathcal{E}}^2 : \rangle = \langle \psi(t) | : \left\{ \sum_m \sqrt{\frac{\hbar \omega_m}{\epsilon_0 V}} (a_m + a_m^\dagger) \times \sin \left[ (m_0 + m) \frac{\pi z}{L} \right] \right\}^2 : | \psi(t) \rangle. \quad (36)$$

In the limit considered in this paper we can replace the frequencies  $\omega_m$  under the radical with the constant  $\omega_1^{(\text{at})}$ . After expanding the state vector as in equation (17), normally ordering the operators, and evaluating the sums, the expectation value can be written in terms of the amplitudes  $b_m(t)$  to find the photon in the various cavity modes

$$\langle : \hat{\mathcal{E}}^2 : \rangle = \left( \frac{2\hbar \omega_1^{(\text{at})}}{\epsilon_0 V} \right) \left| \sum_m b_m(t) \sin \left[ (m_0 + m) \frac{\pi z}{L} \right] \right|^2. \quad (37)$$

Evaluation of this expression gives a space- and time-dependent representation of the localization of the energy of the photon [17, 18].

The expression for  $\langle : \hat{\mathcal{E}}^2 : \rangle$  in equation (37) is the square of a complex number that is analogous to the complex analytic signal describing the classical field. We label this quantity  $\mathcal{E}_{\text{qm}}$ , i.e.

$$\mathcal{E}_{\text{qm}} = \left( \frac{2\hbar \omega_1^{(\text{at})}}{\epsilon_0 V} \right)^{1/2} \sum_m b_m(t) \sin \left[ (m_0 + m) \frac{\pi z}{L} \right]. \quad (38)$$

The overall phase of this quantity is clearly arbitrary; in what follows we retain the phase that comes from a direct evaluation of this equation. As we have previously noted [14] this quantity  $\mathcal{E}_{\text{qm}}$  is very closely related to what has been identified as ‘the ‘electric field’ associated with [a] single photon state’ by Scully and Zubairy [12]. For further discussion of the relationship see [14].

For ease of comparison with previous results for the detector atom, we investigate the field at the fixed position  $z = 3L/4$ . With no scattering atom present we find [14]

$$\mathcal{E}_{\text{qm}}^0 = -i\Theta \left( t - \frac{1}{2} \right) \left( \frac{\hbar \omega_1^{(\text{at})} \gamma_1 \pi}{2\pi \epsilon_0 V \Delta} \right)^{1/2} \exp \left[ -\frac{\gamma_1}{2} \left( t - \frac{1}{2} \right) \right]. \quad (39)$$

The energy density passing the point  $z = 3L/4$  exhibits an abrupt turn-on (because of the initial conditions we have chosen) followed by exponential decay [12, 14, 17, 18]. With a three-level scattering atom present at  $z = L/2$  we find

$$\begin{aligned} \mathcal{E}_{\text{qm}} = & -i\Theta \left( t - \frac{1}{2} \right) \left( \frac{\hbar \omega_1^{(\text{at})} \gamma_1 \pi}{2\epsilon_0 V \Delta} \right)^{1/2} \left\{ \exp \left[ -\frac{\gamma_1}{2} \left( t - \frac{1}{2} \right) \right] \right. \\ & + \frac{\gamma_2(\gamma_1 + i2\delta) \exp \left[ -\frac{\gamma_1}{2} \left( t - \frac{1}{2} \right) \right]}{\gamma_1^2 - \gamma_1 \gamma_2 - 4\delta^2 + \omega_R^2 + i2\delta(2\gamma_1 - \gamma_2)} \\ & + \frac{\gamma_2 \gamma_2'' \exp \left[ -\left( \frac{\gamma_2''}{2} + i\delta \right) \left( t - \frac{1}{2} \right) \right]}{\sqrt{\gamma_2^2 - 4\omega_R^2} (\gamma_1 - \gamma_2'' + i2\delta)} \\ & \left. + \frac{\gamma_2 \gamma_2' \exp \left[ -\left( \frac{\gamma_2'}{2} + i\delta \right) \left( t - \frac{1}{2} \right) \right]}{\sqrt{\gamma_2^2 - 4\omega_R^2} (\gamma_1 - \gamma_2' + i2\delta)} \right\}. \quad (40) \end{aligned}$$

Using only the first term in curly brackets leads to the previous result with no scattering atom present. The steady state scattering is obtained by including the second term in curly brackets. Probability associated with this term decays at the slow rate  $\gamma_1$  reflecting the envelope of the incident radiation. We claimed previously that for large  $\gamma_3$  the detector atom response reflects the field incident upon it, and comparison of equation (31), which gives the probability amplitude due to scattering for the detector atom, with equation (40), justifies this claim. In the limit  $\gamma_3 \gg \gamma_2, \gamma_1$  the factors  $\mathcal{F}_{20}$  through  $\mathcal{F}_{23}$  that arise in equation (31) are proportional to the coefficients in front of the corresponding exponential terms in equation (40).

#### 4. Comparison of semi-classical and quantum mechanical scattering

In the semi-classical model the result of weak scattering of a monochromatic field is contained in equation (4). In the limit of narrow bandwidth probe ( $\gamma_1 \ll \gamma_2$ ) and rapid detector atom response ( $\gamma_3 \gg \gamma_1, \gamma_2$ ) our quantum amplitude for the detector atom to be excited by the scattered field is approximated by the first term of equation (31),

$$\begin{aligned} c_3^s(t) & \simeq -\Theta \left( t - \frac{1}{2} \right) \exp \left[ -\frac{\gamma_1}{2} \left( t - \frac{1}{2} \right) \right] \\ & \times \sqrt{\frac{\gamma_1}{\gamma_3}} \frac{i\delta \gamma_2 / 2}{\omega_R^2 / 4 - \delta^2 - i\delta \gamma_2 / 2} \\ & \simeq c_3^0(t) \frac{i\delta \gamma_2 / 2}{\omega_R^2 / 4 - \delta^2 - i\delta \gamma_2 / 2}. \quad (41) \end{aligned}$$

This has exactly the same functional form as the term due to scattering in the formula for the classical field, equation (4). In the classical formula the dimensionless factor  $f = N \Delta z |d|^2 \omega / (\hbar \epsilon_0 c \gamma)$  is assumed to be small. In our quantum model the magnitude of the scattering is determined by  $\Omega_2$  (or equivalently  $\gamma_2$ ), which characterizes the coupling of atom 2 to the probe field. In our one-dimensional model the coupling to the incident field and the decay rate of atom 2 are both

completely determined by the single parameter  $\Omega_2$ , which means that it is not possible to make the effect of the scattering small without simultaneously making the line-width of atom 2 very narrow. In a fully three-dimensional model the decay rate of atom 2 would be the result of the atom's coupling to many more modes, and not just those containing the incident field. This scattering into other modes would reduce the scattering in the forward direction (the direction of the detector) from the amount predicted in our simple model. If the forward scattering is reduced by a factor  $f$ , then a more realistic expression for the excitation of the detector atom is

$$c_3(t) = c_3^0(t) + f c_3^s(t). \quad (42)$$

We have used the same symbol  $f$  here that we used for the dimensionless parameter which characterizes the magnitude of classical scattering in order to emphasize the analogy between the quantum superposition of equation (42) and the classical field superposition of equation (4).

Returning to field quantities, the quantum pulse of equation (39) has the classical analogue

$$\mathcal{E}_{\text{cl}}^0 = \Theta\left(t - \frac{1}{2}\right) C \exp\left[-\left(\frac{\gamma_1}{2} + i\omega_1\right)\left(t - \frac{1}{2}\right)\right], \quad (43)$$

where  $C$  is a constant. If such classical pulses are incident on a thin slab of material with thickness  $\Delta z$ , density  $N$ , and classical susceptibility  $\chi$  given by equation (1), then the classical transmitted field  $\mathcal{E}_{\text{cl}}$  is identical in form to equation (40), except that the terms due to scattering (i.e. those proportional to  $\gamma_2$ ) have a magnitude characterized by the classical dimensionless factor  $N\Delta z|d|^2\omega/(\hbar\epsilon_0 c\gamma_2)$ . A derivation of this result is included in an appendix.

## 5. Temporal-centre-of-gravity delay

The group velocity of a classical field has a clear interpretation for quasi-monochromatic fields: it is the speed at which the peak of the modulation envelope travels. Group delays refer to the delay in the arrival of the peak of a pulse compared to the time expected for propagation through a vacuum. The pulses investigated in this paper have sharp leading edges, and this lack of a smooth modulation envelope means that the results of simple classical theory for quasi-monochromatic pulses should not be expected to be a sufficient guide to full understanding. In this section we will investigate 'temporal-centre-of-gravity' delays in several classical and quantum mechanical quantities.

The first delay we investigate is derived from  $c_3(t)$ , the amplitude for the detector atom to be excited. As we have argued previously, this amplitude reflects the strength of the incident field in the limit that the response time of this atom is very short compared with other timescales, i.e.  $\gamma_3 \gg \gamma_1, \gamma_2$ . The effect of the scattering on this amplitude is evident in figure 6, in which  $|c_3(t)|^2$ , the probability for the detector atom to be excited, is plotted for three values of the detuning  $\delta$ , and also for the case in which no scattering atoms are present. For clarity in this figure we have only included the terms corresponding to the initial 'turn-on' of the excitation; we have not included effects due to reflection and multiple scattering. (The results are plotted for the specific case in which  $\omega_R = \gamma_2/2$ .) For all detunings,  $c_3(t) = 0$  for all times earlier than

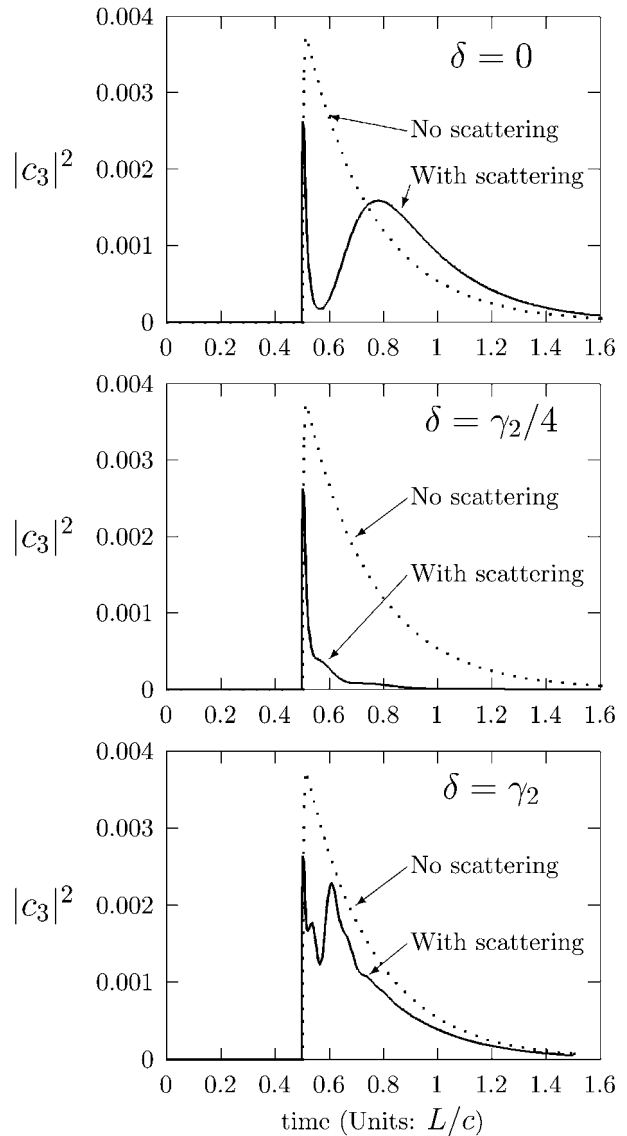


**Figure 6.** Probability for the detector atom to be excited as a function of time for various values of the detuning  $\delta$ . (All effects due to multiple scattering and reflections have been suppressed.) The effect of the 'pulse reshaping' is dependent on the detuning. The temporal centre-of-gravity of the probability is shifted relative to that in the case of no scattering from relatively late times in the top graph to earlier times in the middle two graphs, and then back to later times in the bottom graph. The decay rates of the atoms are  $\gamma_1 = 4$ ,  $\gamma_2 = 64$ , and  $\gamma_3 = 1024$  in the units of the figure; the Rabi frequency of the B–C transition of atom 2 is  $\omega_R = \gamma_2/2 = 32$ .

$t = 0.5L/c$ , as is expected; all effects on the detector atom occur at times that preserve causality. The qualitative shapes of the detector response depend critically on the detuning  $\delta$ . For  $\delta = 0$  the steady-state absorption coefficient is zero, and this is reflected in the fact that at large times there is little effect of the scattering on the probability. At earlier times the effects of transient oscillations are pronounced, and the detector response as reflected in the shape of  $|c_3(t)|^2$  is shifted toward later times relative to the response with no scattering atom present. The response shifts to earlier times as the detuning is increased, and for values in the vicinity of  $|\delta| = \gamma_2/4$  it occurs earlier than the in the case of no scattering. This is the region in which

negative values of the group delay occur, as is illustrated in figure 2. The finite response time of the medium results in large brief transmission of the leading edge of the pulse of the field before the high attenuation of the steady state sets in. (A similar effect occurs in resonant scattering from simple two-level atoms [14].) At larger detuning values, such as the case  $\delta = \gamma_2$  illustrated in the bottom graph of figure 6, most of the probability is again removed at early times, shifting the overall response back to later times.

We quantify the ideas illustrated in figure 6 by identifying an effective arrival time of the photon with the temporal centre-of-gravity of the probability that the detector atom is excited, i.e.

$$t_{\text{arrival}} = \frac{\int t |c_3(t)|^2 dt}{\int |c_3(t)|^2 dt}. \quad (44)$$

The delay imposed by the medium is then just the difference in the arrival times calculated with and without a scattering atom present,

$$\Delta t_{c_3} = \frac{\int t |c_3(t)|^2 dt}{\int |c_3(t)|^2 dt} - \frac{\int t |c_3^0(t)|^2 dt}{\int |c_3^0(t)|^2 dt}. \quad (45)$$

To explore the effect of weak scattering we rewrite  $c_3(t)$  in the form of equation (42), and assume that  $f \ll 1$ . To first order in  $f$  our quantum mechanical delay becomes

$$\begin{aligned} \Delta t_{c_3} &= \frac{\int t |c_3^0(t) + f c_3^s(t)|^2 dt}{\int |c_3^0(t) + f c_3^s(t)|^2 dt} - \frac{\int t |c_3^0(t)|^2 dt}{\int |c_3^0(t)|^2 dt} \\ &\simeq 2f \left[ \frac{\int t \operatorname{Re}[c_3^0(t) c_3^s(t)^*] dt}{\int |c_3^0(t)|^2 dt} \right. \\ &\quad \left. - \frac{\int t |c_3^0(t)|^2 dt \int \operatorname{Re}[c_3^0(t) c_3^s(t)^*] dt}{(\int |c_3^0(t)|^2 dt)^2} \right]. \quad (46) \end{aligned}$$

It is straightforward (but involved) to evaluate the integrals in equation (46) using the expressions for  $c_3^0(t)$  and  $c_3^s(t)$  from equations (30) and (31). After taking the limit  $\gamma_3 \rightarrow \infty$  and then letting  $\gamma_1 \rightarrow 0$  we arrive at the following expression for the quantum time delay:

$$\Delta t_{c_3} = 4f\gamma_2 \frac{(\omega_R^2 + 4\delta^2)[(\omega_R^2 - 4\delta^2)^2 - 4\gamma^2\delta^2]}{[(\omega_R^2 - 4\delta^2)^2 + 4\gamma^2\delta^2]}. \quad (47)$$

Comparing this to equation (6) shows that the ‘temporal-centre-of-gravity’ delay time for this specific pulse is identical in functional form to the classical group delay given in the equation. The magnitude of the temporal-centre-of-gravity delay is, however, twice that given by the group delay. (The temporal-centre-of-gravity delay for classical pulses with the form given in equation (43) is also twice as large as the group delay.) The difference in the classical group delay and the temporal-centre-of-mass delay should not be surprising, because the pulses studied in this paper do not satisfy the quasi-monochromatic condition.

The delay in the arrival time that we have defined is the result of the reshaping of the ‘pulse’ of excitation of the detector atom. The effect of scattering in the region of resonance is effectively to redistribute (in time) the probability that the detector atom will be excited. The scattering atom can rapidly absorb energy from the probe field, and the coupling field creates a state of the system which can then return energy

to the probe field at a rate which can be adjusted, via the Rabi frequency  $\omega_R$ , to be arbitrarily slow. Although we have not demonstrated it explicitly in this work, we are confident that delays in the quasi-monochromatic quantum pulses with smooth envelopes can be explained in the same manner.

As  $\mathcal{E}_{cl}$ ,  $\mathcal{E}_{qm}$ , and  $c_3(t)$  all have the same functional form (in the large  $\gamma_3$  limit), it is easy to see that equivalent delays can be derived from the classical field using equation (7), or from the quantum field using the analogous equation

$$\begin{aligned} \Delta t_{(\mathcal{E}^2)} &= \left( \frac{\int t \langle \hat{\mathcal{E}}(z = 3L/4)^2 \rangle dt}{\int \langle \hat{\mathcal{E}}(z = 3L/4)^2 \rangle dt} \right)_{\text{with scatterer}} \\ &\quad - \left( \frac{\int t \langle \hat{\mathcal{E}}(z = 3L/4)^2 \rangle dt}{\int \langle \hat{\mathcal{E}}(z = 3L/4)^2 \rangle dt} \right)_{\text{no scatterer}}. \quad (48) \end{aligned}$$

## 6. Conclusion

We have considered a fully quantized model of scattering by three-level atoms which can exhibit electromagnetically induced transparency. Our model is simple enough that we are able to find an analytical solution describing the complete dynamics of the system. Using this model we have investigated the propagation of single spontaneously emitted photons through a medium exhibiting electromagnetically induced transparency, and have defined an effective time of arrival at a detector atom. We have also calculated the expectation value of the field intensity operator, and identified a quantum analogue to the complex analytic signal describing the classical field. These quantum mechanical quantities exhibit delays that are clearly the result of pulse-reshaping effects. We have compared our delays for quantized one-photon fields with those calculated for classical fields using the index of refraction determined from semi-classical theory, and find them to be in agreement. As in our previous work [14] the effect of the fields on the atoms and the atoms on the field have exact analogues in the effects predicted by semi-classical theories. This work provides a further example of how phase shifts imposed on a classical field are manifested in a quantized version of the theory.

## Acknowledgments

TP acknowledges support from the National Science Foundation Research Experiences for Undergraduates Programme (NSF Grant no PHY-0097424).

## Appendix A. Solution using Laplace transforms

Taking the Laplace transform of the coupled differential equations (18)–(22) gives the coupled algebraic equations

$$i(s\tilde{c}_1(s) - 1) = \sum_m g_{1m} \tilde{b}_m(s), \quad (A.1)$$

$$(is + \delta)\tilde{c}_2(s) = \sum_m g_{2m} \tilde{b}_m(s) + \omega_R \tilde{d}(s)/2, \quad (A.2)$$

$$is\tilde{c}_3(s) = \sum_m g_{3m} \tilde{b}_m(s), \quad (A.3)$$

$$is\tilde{d}(s) = \omega_R \tilde{c}_2(s)/2 - \delta\tilde{d}(s), \quad (A.4)$$

$$is\tilde{b}_m(s) = \sum_j g_{jm}^* \tilde{c}_j(s) + m\Delta\tilde{b}_m(s). \quad (\text{A.5})$$

We solve these algebraic equations for the quantities  $\tilde{c}_j(s)$ ,  $\tilde{d}(s)$ , and  $\tilde{b}_m(s)$ , and then perform an inverse Laplace transform to recover the time dependence of  $c_j(t)$ ,  $d(t)$ , and  $b_m(t)$ . The details of carrying out such calculations are quite involved, and were completed with the aid of a computer algebra system<sup>5</sup>. In this appendix we outline our approach and present some of our intermediate results.

We begin by solving equation (A.4) for  $\tilde{d}(s)$  and (A.5) for  $\tilde{b}_m(s)$ , and substitute the results in the first three equations, giving

$$s\tilde{c}_1 - 1 = -i\Delta(f_{11}\tilde{c}_1 + f_{12}\tilde{c}_2 + f_{13}\tilde{c}_3), \quad (\text{A.6})$$

$$\tilde{c}_2 = -i\Delta(f_{12}\tilde{c}_1 + f_{22}\tilde{c}_2 + f_{23}\tilde{c}_3) \left[ \frac{4(s - i\delta)}{4(s - i\delta)^2 + \omega_R^2} \right], \quad (\text{A.7})$$

$$s\tilde{c}_3 = -i\Delta(f_{13}\tilde{c}_1 + f_{23}\tilde{c}_2 + f_{33}\tilde{c}_3), \quad (\text{A.8})$$

in which we have defined the dimensionless sums

$$f_{ln} = \frac{1}{\Delta^2} \sum_m \frac{g_{ln}g_{mn}^*}{\frac{is}{\Delta} - m}. \quad (\text{A.9})$$

In the limit in which the atomic resonance frequencies are very much greater than the fundamental frequency of the cavity, i.e.  $\omega_j^{(\text{at})} \gg \Delta$ , these sums may be approximated by extending the range for  $m$  from  $-\infty$  to  $+\infty$ , in which case the sums have relatively simple representations in terms of trigonometric functions. An example of the explicit form of such sums is given in the appendix of [14].

After solving equations (A.6)–(A.8) for the quantities  $\tilde{c}_j(s)$  in terms of the sums  $f_{jm}$ , we rewrite the hyperbolic trigonometric functions resulting from the sums in terms of exponential functions, and expand the resulting expressions in powers of  $\exp(-s/2)$  or  $\exp(-s/4)$ . We also let  $c/L = 1$  at this point in the calculation. The time dependence of the system is recovered by a term-by-term inverse Laplace transform of the expansion. The step function turn-on of the resulting time dependence arises because of the factors  $\exp(-ns/4)$  in the expansion. The lowest order terms in our expansions of the Laplace transforms are given here

$$\begin{aligned} \tilde{c}_1(s) &= \frac{2}{2s + \gamma_1} \\ &+ \frac{2 \exp(-s/2) \gamma_1 [4s^2 + 4s\gamma_2 - 4\delta^2 + \omega_R^2 - 4i\delta(2s + \gamma_2)]}{(2s + \gamma_1)^2 [4s^2 + 2s(\gamma_2 - i4\delta) - i2\gamma_2\delta - 4\delta^2 + \omega_R^2]} \\ &+ \dots, \end{aligned} \quad (\text{A.10})$$

$$\begin{aligned} \tilde{c}_2(s) &= -\frac{4 \exp(-s/4) \sqrt{\gamma_1 \gamma_2} (s - i\delta)}{(2s + \gamma_1) [4s^2 + 2s\gamma_2 - 4\delta^2 + \omega_R^2 - i2\delta(4s + \gamma_2)]} \\ &+ \dots, \end{aligned} \quad (\text{A.11})$$

$$\begin{aligned} \tilde{c}_3(s) &= -\frac{2 \exp(-s/2) \sqrt{\gamma_1 \gamma_3} (4s^2 - 4\delta^2 + \omega_R^2 - i8s\delta)}{(2s + \gamma_1)(2s + \gamma_3) [4s^2 + 2s\gamma_2 - 4\delta^2 + \omega_R^2 - i2\delta(4s + \gamma_2)]} \\ &+ \dots, \end{aligned} \quad (\text{A.12})$$

<sup>5</sup> Mathematica notebooks used to perform the calculations are available from the authors.

$$\begin{aligned} \tilde{d}(s) &= \frac{i2 \exp(-s/4) \sqrt{\gamma_1 \gamma_2} \omega_R}{(2s + \gamma_1) [4s^2 + 2s\gamma_2 - 4\delta^2 + \omega_R^2 - i2\delta(4s + \gamma_2)]} \\ &+ \dots, \end{aligned} \quad (\text{A.13})$$

$$\begin{aligned} \tilde{b}_m(s) &= -\frac{i2g_{1m}}{(s + im\pi)(2s + \gamma_1)} \\ &+ \frac{i4 \exp(-s/4) \sqrt{\gamma_1 \gamma_2} (s - i\delta) g_{2m}}{(s + im\pi)(2s + \gamma_1) [4s^2 + 2s\gamma_2 - 4\delta^2 + \omega_R^2 - i2\delta(4s + \gamma_2)]} \\ &+ \dots. \end{aligned} \quad (\text{A.14})$$

The inverse Laplace transform of these expressions gives equations (24)–(28).

## Appendix B. Classical scattering of exponential pulses

A general pulse  $E(z, t)$  may be written in terms of its Fourier transform as

$$E(z, t) = \frac{1}{\sqrt{2\pi}} \int_{-\infty}^{\infty} A(\omega) \exp[i\{m(\omega)z - \omega t\}] d\omega, \quad (\text{B.1})$$

where

$$A(\omega) = \frac{C}{\sqrt{2\pi}} \int_{-\infty}^{\infty} E(0, t) \exp(i\omega t) dt. \quad (\text{B.2})$$

We consider an incident pulse like that of equation (43) which for convenience we consider to arrive at the origin  $z = 0$  at  $t = 0$ . The Fourier transform of this pulse is

$$A(\omega) = \frac{C}{\sqrt{2\pi}} \frac{1}{[\gamma_1/2 - i(\omega - \omega_1)]}. \quad (\text{B.3})$$

The effect of weak scattering on a Fourier component of a plane wave is contained in equation (4), and we construct the transmitted pulse to the right of the scattering region from the original Fourier components appropriately modified according to this equation. For weak scattering the dimensionless parameter  $f = N\Delta z|d|^2\omega/(\hbar\epsilon_0 c\gamma_2)$  is small, and the transmitted field is thus

$$\begin{aligned} E_t(z, t) &= \frac{1}{\sqrt{2\pi}} \int_{-\infty}^{\infty} A(\omega) \exp[i\omega(z/c - t)] \\ &\times \left[ 1 + if \frac{\delta\gamma_2/2}{\omega_R^2/4 - \delta^2 - i\delta\gamma_2/2} \right] d\omega \\ &= \frac{C}{2\pi} \int_{-\infty}^{\infty} \frac{\exp[i\omega(z/c - t)]}{[\gamma_1/2 - i(\omega - \omega_1)]} \\ &\times \left[ 1 + if \frac{(\omega - \omega_2)\gamma_2/2}{\omega_R^2/4 - (\omega - \omega_2)^2 - i(\omega - \omega_2)\gamma_2/2} \right] d\omega \\ &= E_i(z, t) + \frac{iCf\gamma_2}{4\pi} \times \int_{-\infty}^{\infty} \frac{\exp[i\omega(z/c - t)]}{[\gamma_1/2 - i(\omega - \omega_1)]} \\ &\times \left[ \frac{(\omega - \omega_2)}{\omega_R^2/4 - (\omega - \omega_2)^2 - i(\omega - \omega_2)\gamma_2/2} \right] d\omega. \end{aligned} \quad (\text{B.4})$$

The integrand of this expression has three poles, all of which lie in the lower half of the complex plane. For  $(z/c - t) > 0$  the integration along the real axis is closed in the upper-half plane, giving a result of zero. For  $(z/c - t) < 0$  the contour is closed in the lower half plane encircling the poles, giving a result that is identical in form to the quantum mechanical expression equation (40). (The factor  $\exp(-i\omega_1 t)$  does not appear in equation (40) because of the zero chosen for the energy scale in the quantum calculations.)

## References

- [1] Scully M O 1991 *Phys. Rev. Lett.* **67** 1855
- [2] Bollor K-J, Imamoğlu A and Harris S E 1991 *Phys. Rev. Lett.* **66** 2593
- [3] Field J E, Hahn K H and Harris S E 1991 *Phys. Rev. Lett.* **67** 3062
- [4] Harris S E, Field J E and Kasapi A 1992 *Phys. Rev. A* **46** R29
- [5] Hau L V, Harris S E, Dutton Z and Behroozi C H 1999 *Nature* **397** 594
- [6] Kash M M, Sautenkov V A, Zibrov A S, Hollberg L, Welch G R, Lukin M D, Rostovtsev Y, Fry E S and Scully M O 1999 *Phys. Rev. Lett.* **82** 5229
- [7] Wang L J, Kuzmich A and Dogariu A 2000 *Nature* **406** 277
- [8] Dogariu A, Kuzmich A and Wang L J 2001 *Phys. Rev. A* **63** 053806
- [9] Lukin M and Imamoğlu A 2001 *Nature* **413** 273
- [10] Harris S E 1997 *Phys. Today* **50** 36
- [11] Lukin M, Yellin S, Zibrov A and Scully M 1999 *Laser Phys.* **9** 759
- [12] Scully M O and Zubairy M S 1997 *Quantum Optics* (Cambridge: Cambridge University Press)
- [13] Feynman R P, Leighton R B and Sands M 1963 *The Feynman Lectures on Physics* vol 1 (Reading, MA: Addison-Wesley) ch 31 and 32
- [14] Purdy T, Taylor D F and Ligare M 2003 *J. Opt. B: Quantum Semiclass. Opt.* **5** 85
- [15] Taylor D F 2001 Undergraduate Honors Thesis Bucknell University
- [16] Ligare M and Taylor D F 2001 *Eighth Rochester Conf. on Coherence and Quantum Optics* (New York: Plenum) at press  
<http://www.eg.bucknell.edu/physics/ligare.html/>
- [17] Ligare M and Oliveri R 2002 *Am. J. Phys.* **70** 58
- [18] Bužek V, Drobný G, Kim M G, Havukainen M and Knight P L 1999 *Phys. Rev. A* **60** 582
- [19] Smith R L 1970 *Am. J. Phys.* **38** 978
- [20] Bloch S C 1977 *Am. J. Phys.* **45** 538
- [21] Meystre P and Sargent M 1999 *Elements of Quantum Optics* 3rd edn (Berlin: Springer)
- [22] Stey G C and Gibberd R W 1972 *Physica* **60** 1
- [23] Milonni P W and Knight P L 1974 *Phys. Rev. A* **10** 1096
- [24] Milonni P W and Knight P L 1975 *Phys. Rev. A* **11** 1090
- [25] Gießen H, Berger J D, Mohs G and Meystre P 1996 *Phys. Rev. A* **53** 2816